Magnetic flux loss from interstellar clouds

Toyoharu Umebayashi
Data Processing Center, Yamagata University, Yamagata 990, Japan

Takenori Nakano
Department of Physics, Kyoto University, Sakyo-ku, Kyoto 606, Japan

SUMMARY

The densities of charged particles in ionization–recombination equilibrium are investigated with some revised reaction rate coefficients. Especially the dissociative recombination rate of H_3^+ with an electron is decreased by a factor 10^2 compared with the rate generally used before. At the density by hydrogen number $n_H \lesssim 10^{11}$ cm^{-3}, where electrons and ions are the dominant charged particles, the ionization fraction depends considerably on the degree of depletion of heavy elements from the gas phase. At higher densities where grains are the dominant charged particles, the abundances of some dominant charged particles depend scarcely on the degree of the element depletion. Dissipation of magnetic fields due to plasma drift (ambipolar diffusion) and ohmic loss is investigated for the cloud cores with density $n_H \approx 10^3$–10^{13} cm^{-3}. At $n_H \lesssim 10^{11}$ cm^{-3} the dissipation time of magnetic fields is considerably greater than the free-fall time, and it is difficult to decrease the magnetic flux of the cloud core much below the critical flux for magnetohydrostatic equilibrium. At $n_H \gtrsim$ several $\times 10^{11}$ cm^{-3} the magnetic field decouples from the gas due to ohmic dissipation, and only a nearly uniform field can exist in such a cloud.

1 INTRODUCTION

The magnetic flux problems in star formation can be classified into two categories. First, the magnetic field may inhibit the contraction of the cloud. An interstellar cloud is supported by the magnetic force against the self-gravity when its magnetic flux Φ is greater than the critical flux given by

$$\Phi_c \approx 2\pi G^{1/2} M, \qquad (1)$$

where G is the gravitational constant and M is the mass of the cloud (Mestel 1965, 1966; Strittmatter 1966; Field 1970; Nakano 1981, 1984). A cloud (or a part of the cloud) cannot form stars unless its flux is decreased below Φ_c. Secondly, the magnetic flux through an ordinary cloud is not much less than Φ_c, and the magnetic flux-to-mass ratio of the cloud exceeds the ratio of the magnetic star by a factor of between several hundred and 10^5 (Nakano 1983a, 1984). Thus, most of the initial flux of the cloud (or more exactly the cloud core) must be lost at some stage of star formation.

The magnetic field in a slightly ionized cloud dissipates by the process referred to alternatively as 'ambipolar diffusion' or 'plasma drift' (Mestel & Spitzer 1956) and by the ohmic dissipation. Although both processes operate simultaneously, the latter is negligible in the cloud of ordinary density. Nakano & Umebayashi (1986a,b) formulated a method of treating both processes simultaneously and found that the magnetic field decouples from the gas only at the hydrogen number density $n_H \gtrsim$ several $\times 10^{11}$ cm^{-3} where the ohmic dissipation is the dominant process.

The dissipation of magnetic fields depends strongly on the densities of various charged particles. By laboratory experiments Smith & Adams (1984) found only an upper limit to the rate coefficient of the dissociative recombination of H_3^+ with a free electron, which is two orders of magnitude smaller than the coefficient generally used before. Amano's (1988) experiments show the rate coefficient nearly equal to the old value. Thus the recombination of H_3^+ is controversial at present. Because H_3^+ may be a dominant charged particle in some situations, this may have significant effects on the magnetic flux loss. There have been some other revisions on the reaction rate coefficients. The purpose of this paper is to re-investigate the dissipation of magnetic fields in the interstellar clouds with the new rate coefficients.

In Section 2 we investigate the densities of various charged particles in the ionization–recombination equilibrium with a simplified reaction scheme. Using the general formula for describing the dissipation of magnetic fields we investigate in Section 3 the time-scale of magnetic flux loss from the cloud cores with n_H between 10^3 and 10^{13} cm^{-3}. Some related

problems are discussed in Section 4. Results obtained in this paper are summarized in Section 5.

2   DENSITIES OF CHARGED PARTICLES

Oppenheimer & Dalgarno (1974) investigated the fractional ionization in dense interstellar clouds. A simplified reaction scheme including the grain surface recombinations for calculating the densities of various charged particles was constructed by Nakano (1976) and was reinforced by Umebayashi & Nakano (1980). Umebayashi (1983) and Nakano (1984) also investigated the densities of charged particles in a cloud of higher density. In this section we present the model of the reaction scheme with some modifications and investigate the densities of charged particles in various situations of interstellar clouds.

2.1   The simplified reaction scheme

In the magnetic flux problem we need only the densities of some dominant charged particles. The elements to be considered for this purpose are H, He, C, O and refractory heavy elements. The relative abundances of these elements adopted in this paper are shown in Table 1. They are the latest solar abundances (Cameron 1982) except for He the abundance of which is, as in previous work, taken higher than the solar abundance in accordance with the interstellar abundance. The other elements are minor in abundances or do not play an important role in the reaction scheme (e.g. nitrogen). We define two parameters representing the fractions of the elements in the gas phase: δ_1 for the volatile elements C and O, and δ_2 for the refractory heavy metal atoms. As found with extensive measurements of ultraviolet interstellar absorption lines, these heavy elements are considerably depleted in some interstellar clouds compared with the solar abundances (e.g. Morton 1974).

The chemical species included in the reaction scheme are also shown in Table 1. Because we consider dense clouds in which star formation may occur, we assume that most of the elements have been transformed into their molecular form. The oxygen in the gas phase other than the constituent of CO is in the form of O_2, H_2O, OH or O. Because the reaction

rate coefficients of O_2, H_2O and OH with ions are of the same order and the recombination rate coefficients of the resultant ions with electrons are also of the same order, we regard the reactions of the most abundant species O_2 as representative of their reactions. We introduce a parameter f_{O_2} representing the fraction of oxygen in the gas phase in the form of O_2, H_2O or OH. Because the metal atoms Na, Mg, Al, Ca, Fe and Ni have nearly the same rate coefficients for the charge-transfer reactions with ions and the resultant metal ions also have similar rate coefficients for the radiative recombinations with electrons, we neglect the differences among them and denote them as M collectively.

As for the abundance and the size of dust grains we adopt the following simplified model:

(i) all grains have the same radius a. We consider three cases $a \approx 0.3, 0.1$ and $0.03 \, \mu m$,

(ii) grains consist of rocky and metallic materials such as MgO, SiO_2, FeO, NiO, Na, Al and Ca.

Because most of the elements Mg, Si, Fe, Ni, Na, Al and Ca are greatly depleted from the gas phase even in diffuse clouds (e.g. Morton 1974), the grain abundance n_g/n_H by number relative to hydrogen is determined by assuming that the total amount of those elements is in grains. In dense clouds where the temperature is low, grains also contain icy materials such as H_2O, CH_4 and NH_3. We shall investigate in Section 4 the effect of the icy materials on the densities of charged particles and on the dissipation of magnetic fields.

The following species of charged particles are considered in our simplified reaction scheme: electron e, H^+, He^+, C^+, H_3^+, molecular ion m^+ (except H_3^+), metal ion M^+, and grains $G(-1)$ and $G(+1)$ with electric charge $-e$ and e, respectively, where e is the unit electric charge. The important reactions of molecular ions are the charge transfer with metal atoms and the dissociative recombination with electrons. Because the rate coefficients of both reactions are similar among various molecular ions, we neglect the differences among them and denote them as m^+ collectively. Because O^+ reacts rapidly with H_2 to form OH^+, we regard the formation of O^+ as the formation of a molecular ion. Because grains of higher electric charge are scarce in the physical situations of dense clouds and the reaction rate coefficients on grain surface hardly depend on the kind of adsorbed particles (Umebayashi & Nakano 1980; Umebayashi 1983), we consider only the grains of charge $\pm e$ and 0 (neutral) and regard adsorbed ions as a single species.

In dense clouds shielded from the interstellar ultraviolet radiation, the gas is mainly ionized by cosmic rays and radioactive elements. Table 2 lists the reaction rates of H_2 and He with such energetic particles in units of the total ionization rate ζ of a hydrogen molecule, which includes the ionization by secondary electrons. Since H_2^+ reacts immediately with H_2

Table 1. The relative abundances of the elements.

Element	Abundance	Chemical species	Fraction in the gas phase
H	1	H_2	1
He	8.5×10^{-2}	He	1
C	4.2×10^{-4}	CO	δ_1
O	6.9×10^{-4}	O_2, O	δ_1
Metal total	8.4×10^{-5}	M	δ_2
Na	2.3×10^{-6}	Na	δ_2
Mg	4.0×10^{-5}	Mg	δ_2
Al	3.2×10^{-6}	Al	δ_2
Ca	2.3×10^{-6}	Ca	δ_2
Fe	3.4×10^{-5}	Fe	δ_2
Ni	1.8×10^{-6}	Ni	δ_2
Si	3.8×10^{-5}	–	–

Table 2. The ionization rates by energetic particles.

Reaction					Rate
H_2	$\rightarrow$	H_2^+	+ e		0.97ζ[†]
H_2	$\rightarrow$	H^+	+ H	+ e	0.03ζ
He	$\rightarrow$	He^+	+ e		0.84ζ

[†] ζ is the total ionization rate of a hydrogen molecule.

to form H_3^+, we regard H_3^+ as a direct product of the ionization.

The reactions of ions in the gas phase and their rate coefficients are shown in Table 3. We have revised some of the rate coefficients mainly according to the data summarized by Prasad & Huntress (1980). For the rate coefficients of m^+ we use those of the most abundant molecular ion HCO^+. Similarly we use those of Mg^+ for M^+. The dissociative recombination rate coefficient for H_3^+ has been remarkably changed. Smith & Adams (1984) found from laboratory experiments that its rate coefficient in dense clouds is less than $\sim 2 \times 10^{-8}$ cm^3 s^{-1}. Michels & Hobbs (1984) estimated theoretically that for interstellar conditions the H_3^+ recombination rate coefficient is two orders of magnitude smaller than the value generally accepted before. Therefore we use this upper limit in the following calculation. Because we are concerned with the clouds of hydrogen density $n_H \lesssim 10^{13}$ cm^{-3}, we neglect the three-body reactions whose rate coefficients are of the order of 10^{-29} cm^6 s^{-1} (Capone *et al.* 1976).

In addition to the above processes we consider the recombination of ions and electrons on grain surfaces. We adopt the following model for the grain surface reactions (Umebayashi & Nakano 1980; Umebayashi 1983).

(i) When an electron hits a neutral grain, it sticks to the grain with the probability S_e which is between 0.1 and 1.0. When an ion hits a neutral grain, it sticks to the grain without fail.

(ii) When an ion hits a negatively charged grain, and when an electron hits a positively charged grain, the electron and the ion recombine and leave the grain surface.

(iii) When grains of opposite charge in thermal Brownian motion collide, they neutralize themselves.

The mean collision rate coefficient $\langle \sigma v \rangle$ of an ion or an electron of mass m and charge q with a grain of radius a and charge le is given by

$$\langle \sigma v \rangle = \pi a^2 \left(\frac{8k_B T}{\pi m} \right)^{1/2} \left(1 - \frac{lqe}{ak_B T} \right) \qquad \text{for } lq \leq 0, \qquad (2)$$

where T and k_B are the gas temperature and the Boltzmann constant, respectively. The mean collision rate coefficient $\langle \sigma v \rangle_{gg}$ of a grain of radius a and charge le with another grain of a' and $l'e$ is given by

$$\langle \sigma v \rangle_{gg} = \pi (a + a')^2 \left(\frac{8k_B T}{\pi \mu_g} \right)^{1/2} \left(1 - \frac{ll'e^2}{(a+a')k_B T} \right)$$

$$\text{for } ll' \leq 0, \qquad (3)$$

where μ_g is the reduced mass of the colliding grains. We neglect the coalescence of grains.

Draine & Sutin (1987) investigated the recombination of charged particles on grains by taking into account the effect of polarization of grains and by introducing a huge amount of very small grains ($a \ll 0.005$ μm), and found that the rare coefficient is about 10^3 times greater than that obtained by Umebayashi & Nakano (1980). Most of this enhancement is due to the introduction of very small grains. We do not consider the effect of polarization because it is not very important for our grain model.

Fig. 1 shows schematically the scheme of chemical reactions described above. The recombination reactions are
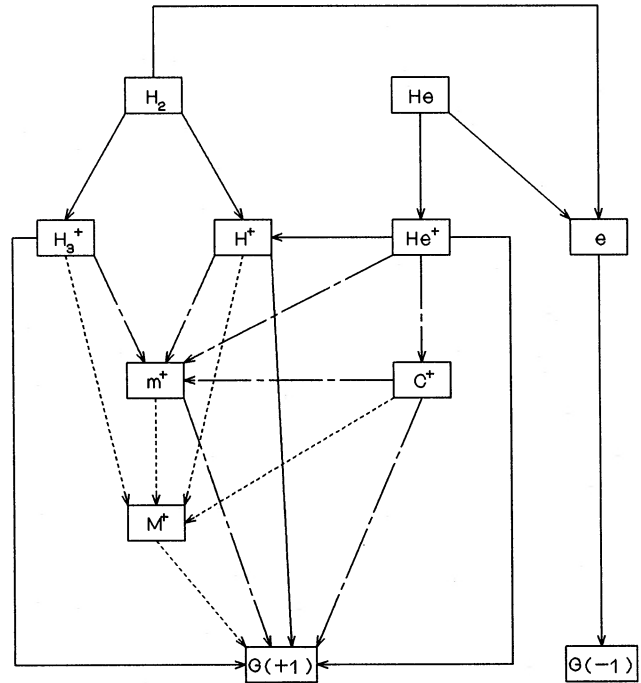
Table 3. The reactions of ions in the gas phase and their rate coefficients.

Reaction								Rate coefficient (cm^3 s^{-1})
H^+	+	O	$\rightarrow$	O^+	+	H		$7.0 \times 10^{-10} \exp(-232/T)$
H^+	+	O_2	$\rightarrow$	O_2^+	+	H		1.2×10^{-9}
H^+	+	M	$\rightarrow$	M^+	+	H		1.1×10^{-9}
He^+	+	H_2	$\rightarrow$	H^+	+	H	$+ \; He$	1.5×10^{-13}
He^+	+	CO	$\rightarrow$	C^+	+	O	$+ \; He$	1.6×10^{-9}
He^+	+	O_2	$\rightarrow$	O^+	+	O	$+ \; He$	1.0×10^{-9}
H_3^+	+	CO	$\rightarrow$	HCO^+	+	H_2		1.7×10^{-9}
H_3^+	+	O	$\rightarrow$	OH^+	+	H_2		8.0×10^{-10}
H_3^+	+	O_2	$\rightarrow$	O_2H^+	+	H_2		6.4×10^{-10}
H_3^+	+	M	$\rightarrow$	M^+	+	H	$+ \; H_2$	1.0×10^{-9}
C^+	+	H_2	$\rightarrow$	CH_2^+	+	$h\nu$		6.0×10^{-16}
C^+	+	O_2	$\rightarrow$	CO^+	+	O		7.5×10^{-10}
C^+	+	O_2	$\rightarrow$	O^+	+	CO		4.1×10^{-10}
C^+	+	M	$\rightarrow$	M^+	+	C		1.1×10^{-9}
m^+	+	M	$\rightarrow$	M^+	+	m		2.9×10^{-9}
H^+	+	e	$\rightarrow$	H	+	$h\nu$		$3.5 \times 10^{-12}(300/T)^{0.7}$
He^+	+	e	$\rightarrow$	He	$.+$	$h\nu$		$4.5 \times 10^{-12}(300/T)^{0.67}$
H_3^+	+	e	$\rightarrow$	H	+	H	$+ \; H$	$\left. \begin{array}{c} \\ \\ \end{array} \right\} \lesssim 2 \times 10^{-8}$
			$\rightarrow$	H_2	+	H		
C^+	+	e	$\rightarrow$	C	+	$h\nu$		$4.4 \times 10^{-12}(300/T)^{0.61}$
m^+	+	e	$\rightarrow$	m_1	+	m_2		$2.0 \times 10^{-7}(300/T)^{0.75}$
M^+	+	e	$\rightarrow$	M	+	$h\nu$		$2.8 \times 10^{-12}(300/T)^{0.86}$

Figure 1. A schematic diagram for the scheme of the chemical reactions related to the densities of charged particles in dense interstellar clouds. Reactions concerning metals and those concerning heavy elements other than metals are shown by the dashed and dot-dashed lines, respectively. The recombination reactions are omitted to avoid the complexity of the figure.

omitted to avoid the complexity of the figure. The reactions concerning metals and those concerning heavy elements other than metals are represented by the dashed lines and the dot–dashed lines, respectively. In the case of no metals in the gas phase ($\delta_2 = 0$), reactions represented by the dashed lines in Fig. 1 are excluded from the reaction scheme. In the case of no heavy elements in the gas phase ($\delta_1 = \delta_2 = 0$), the reaction scheme reduces to the one represented by the solid lines.

2.2   Numerical results

Using the reaction scheme described in Section 2.1, we investigate the densities of charged particles in dense interstellar clouds. The rate equation for constituent X_i is given by

$$\frac{dn(X_i)}{dt} = \sum_j \gamma_{ij}\zeta n(X_j) + \sum_{j,k} \beta_{ijk} n(X_j) n(X_k), \qquad (4)$$

where $n(X_i)$ is the number density of X_i, $\gamma_{ij}\zeta$ is the rate coefficient for forming X_i by the ionization of X_j, and β_{ijk} is the rate coefficient of the two-body reaction. The grain surface reactions are included in the last term. Because the gas in dense clouds is in ionization–recombination equilibrium as will be confirmed in Section 4, we obtain from equation (4)

$$\sum_j \gamma_{ij}\frac{\zeta}{n_H} x(X_j) + \sum_{j,k} \beta_{ijk} x(X_j) x(X_k) = 0, \qquad (5)$$

where $x(X_j) \equiv n(X_j)/n_H$. The fractional abundance $x(X_i)$ of the constituent X_i depends on n_H and ζ through the form n_H/ζ.

We investigate the following cases of the element depletion: (i) $\delta_1 = 0.2$ and $\delta_2 = 0.02$; (ii) $\delta_1 = 0.2$ and $\delta_2 = 0$; (iii) $\delta_1 = \delta_2 = 0$. Case (i) corresponds to the typical diffuse clouds (Morton 1974). Cases (ii) and (iii) are some limiting situations for dense clouds. We take $f_{O_2} = 0.7$ in accordance with the molecular abundances calculated by Mitchell, Ginsburg & Kuntz (1978). We also take $T = 10$ K and $S_e = 1$.

We first take the grain radius $a = 0.1$ μm and the internal density of grains 3 g cm^{-3}. Then we find the relative number density of grains $n_g/n_H \approx 8.9 \times 10^{-13}$. Figs 2–4 show the relative abundances $x(X)$ of various particles X as functions of n_H/ζ. The general features common to the three cases of the element depletion are as follows.

(i) At least at $n_H/\zeta \lesssim 10^{27}$ cm^{-3} s, electrons and ions are the dominant charged particles and more than 70 per cent of grains have an electric charge $-e$ and the rest are mainly neutral.

(ii) At $n_H/\zeta \gtrsim 10^{30}$ cm^{-3} s, grains with charge e and $-e$ are the dominant charged particles and the number density of free electrons is much lower than that of ions.

Some characteristics at the densities where electrons and ions dominate are as follows. In case (i) (Fig. 2) the metal ion M^+ is dominant. This is because M^+ formed by charge transfer from m^+ is destroyed much more slowly than m^+ and the other ions are rapidly transformed into m^+. In case (ii) (Fig. 3) the molecular ion m^+ is dominant. This is because there are no metals in the gas phase and the other ions are
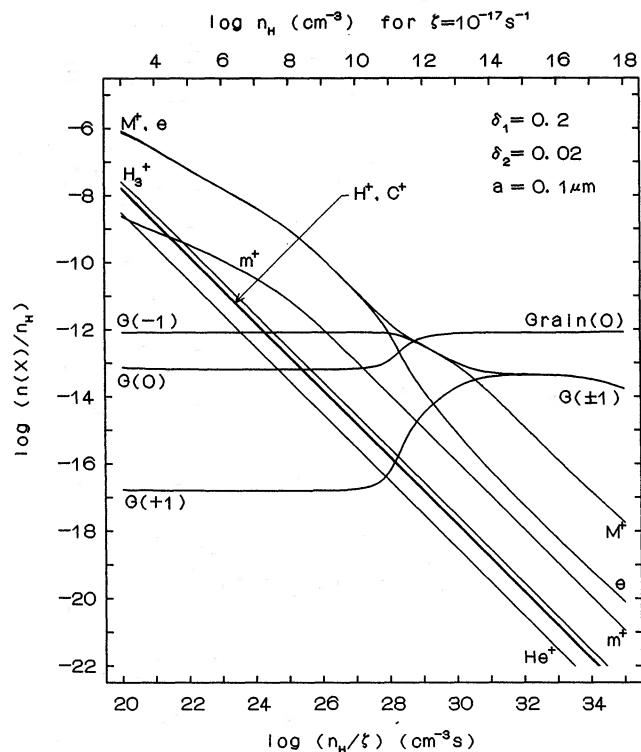

Figure 2. The abundances of various charged particles relative to hydrogen, $n(X)/n_H$, as functions of n_H/ζ, the total hydrogen density n_H divided by the ionization rate of a hydrogen molecule ζ, for the depletion of heavy elements $\delta_1 = 0.2$ and $\delta_2 = 0.02$ and for the grain radius $a = 0.1$ μm. The metal ions, molecular ions other than H_3^+ and the grains with electric charge $-e$, neutral and e are represented as M^+, m^+, $G(-1)$, $G(0)$ and $G(+1)$, respectively.
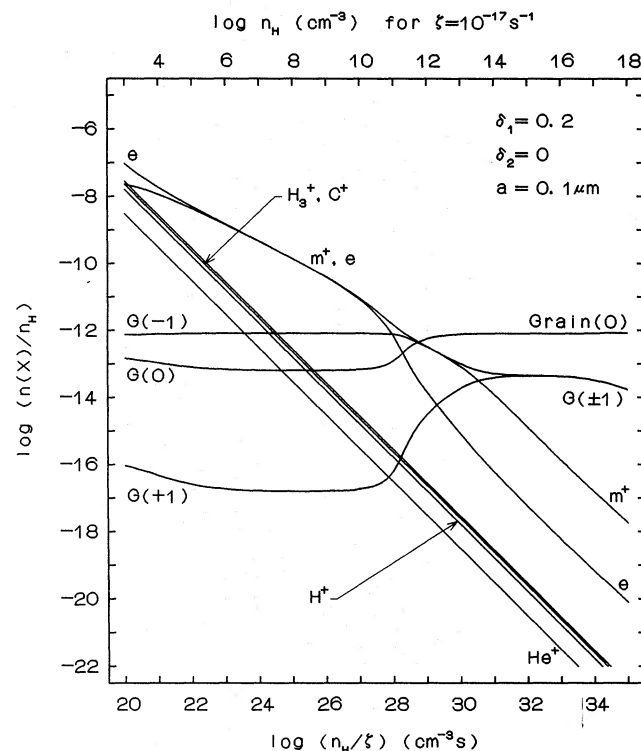

Figure 3. The abundances of various charged particles for $\delta_1 = 0.2$ and $\delta_2 = 0$. The other details are the same as in Fig. 2.

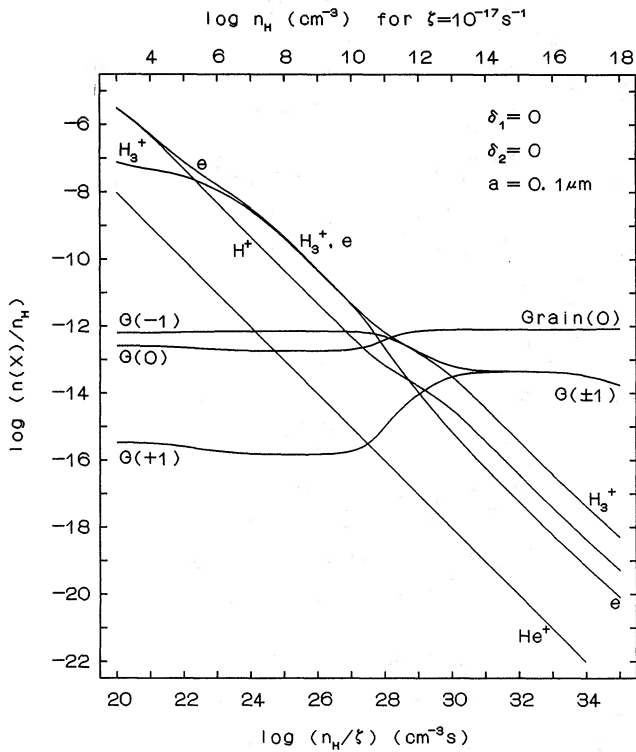log n_H (cm^{-3}) for $\zeta=10^{-17}$s^{-1}

Figure 4. The abundances of various charged particles for $\delta_1 = \delta_2 = 0$. The other details are the same as in Fig. 2.

rapidly transformed into m$^+$. For $\delta_2 \lesssim 10^{-4}$ the abundances of electrons and the dominant ions are nearly the same as in this case with $\delta_2 = 0$. In case (iii) (Fig. 4) H$^+$ is dominant at $n_H/\zeta \lesssim 10^{22}$ cm^{-3} s. Although H$_3^+$ is produced six times more than H$^+$, H$_3^+$ is destroyed much more rapidly through dissociative recombination. At higher n_H/ζ, H$_3^+$ is dominant. This is because the recombination of H$_3^+$ on grains surpasses the dissociative recombination due to the decrease of x(e) and the rate coefficient for the former process is similar to that of H$^+$.

When m$^+$ is destroyed mainly through dissociative recombination [at n_H/ζ less than 10^{25} and 10^{27} cm^{-3} s for cases (i) and (ii), respectively], we approximately have x(e)$\propto$(n_H/ζ)$^{-1/2}$. At $n_H/\zeta > 10^{25}$ cm^{-3} s for case (i) where m$^+$ is destroyed mainly through charge transfer to M and then the ions recombine mainly on grains, we approximately have x(e)$\propto$(n_H/ζ)$^{-1}$. These are the same as in Umebayashi & Nakano (1980). At the densities where H$_3^+$ is dominant in case (iii), we also have x(e)$\propto$(n_H/ζ)$^{-1}$. This is because H$_3^+$ recombines mainly on grains at this density range.

Although the dissociative recombination rate of H$_3^+$ has been decreased by two orders of magnitude compared with the previous works, the densities of charged particles are hardly affected by this in cases (i) and (ii). This is because the transformation of H$_3^+$ into the other molecular ions by the reaction with CO, O$_2$ and O is much faster than the dissociative recombination even with the previously used rate. In case (iii) the recombination of H$_3^+$ occurs mainly on the grain surface at the density region where H$_3^+$ is the dominant ion. The change in the dissociative recombination rate of H$_3^+$ causes the change in the density region where H$_3^+$ is dominant, and therefore the density of free electrons is affected only slightly.

As n_H/ζ increases, the relative abundances of ions decrease, while the abundance of charged grains remains nearly constant as shown in Figs 2–4, and at last at $n_H/\zeta \gtrsim 10^{28}$ cm^{-3} s the number density of grains becomes comparable to or higher than that of ions. In such a situation the number density of electrons is considerably smaller than that of ions because of the charge neutrality. At $n_H/\zeta \gtrsim 10^{30}$ cm^{-3} s the grains with one excess electron and those with one excess ion are dominant charged particles and their number densities become nearly equal to each other.

The charge-state of grains at $n_H/\zeta \gtrsim 10^{30}$ cm^{-3} s depends hardly on the depletion of elements. The relative abundance of electrons is almost the same among the three cases of the element depletion, while there are some differences in the abundance of the dominant ions. As n_H/ζ increases, the ratio of the number densities of electrons and the dominant ions, n_e/n_i, approaches the limiting value

$$\frac{n_e}{n_i} = \left(\frac{1}{S_e}\frac{m_e}{m_i}\right)^{1/2} = \frac{1}{227}\left(\frac{1}{S_e}\frac{28m_H}{m_i}\right)^{1/2}, \qquad (6)$$

where m_e, m_i and m_H are the masses of the electron, ion and hydrogen atom, respectively (Umebayashi 1983; Nakano 1984). Apart from S_e, equation (6) represents the ratio of the collision rate coefficients of ion and electron with neutral grains which are proportional to the thermal velocities of the incoming particles.

Because the recombination of electrons and ions mainly occurs on the grain surface at $n_H/\zeta \gtrsim 10^{27}$ cm^{-3} s, we approximately have x(e)$\propto$(n_H/ζ)$^{-1}$. At 10^{31} cm^{-3} s $\lesssim n_H/\zeta \lesssim 10^{34}$ cm^{-3} s the charge-state of grains hardly changes because it depends only on aT, S_e and n_e/n_i (Umebayashi
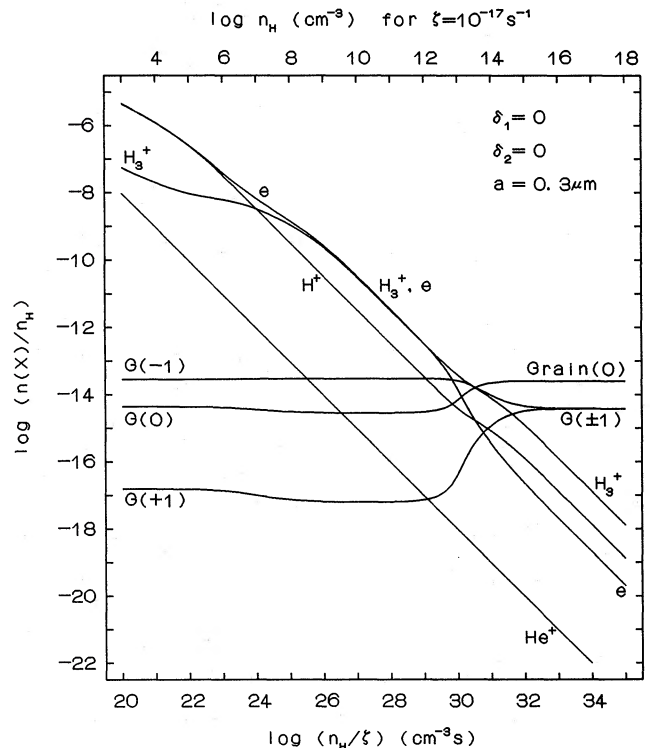
log n_H (cm^{-3}) for $\zeta=10^{-17}$s^{-1}

Figure 5. The abundances of various charged particles for $\delta_1 = \delta_2 = 0$ and for $a = 0.3$ μm. The other details are the same as in Fig. 2.
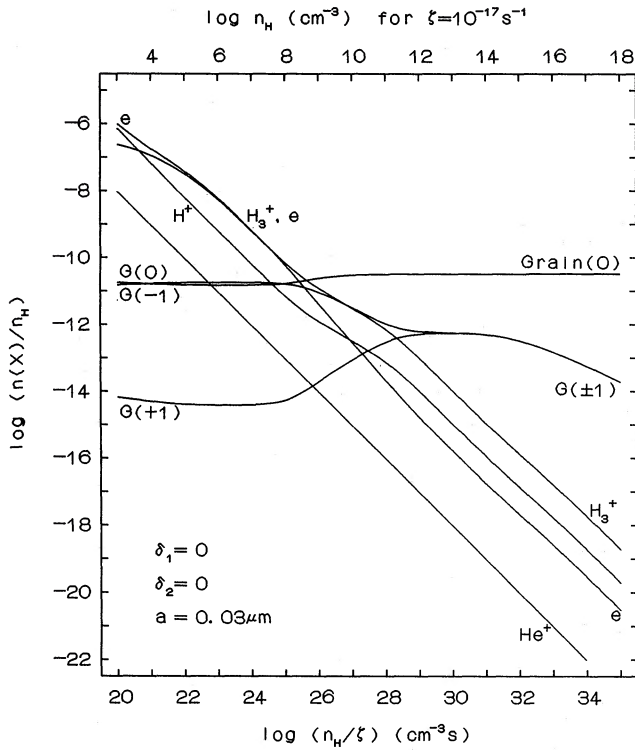
Figure 6. The abundances of various charged particles for $\delta_1 = \delta_2 = 0$ and for $a = 0.03$ μm. The other details are the same as in Fig. 2.

1983). At $n_H/\zeta \gtrsim 10^{34}$ cm^{-3} s recombination of adsorbed electrons and ions during the grain–grain collisions is efficient, and we have $x[G(-1)] \simeq x[G(+1)] \propto (n_H/\zeta)^{-1/2}$.

We next investigate the dependence of $x(X)$ on the grain radius. For $a = 0.3$ and 0.03 μm we have $n_g/n_H \approx 3.3 \times 10^{-14}$ and 3.3×10^{-11}, respectively. The relative abundances $x(X)$ for the case of $\delta_1 = \delta_2 = 0$ are shown in Figs 5 and 6. The results are summarized as follows.

(i) As a increases, the recombination on grain surfaces becomes inefficient and then the relative abundances of electrons and ions increase. This effect is generally larger at higher n_H/ζ, where the grain surface recombination is more efficient than the radiative and dissociative recombinations.

(ii) The value of n_H/ζ at which the number density of grains becomes equal to that of ions is sensitive to a. This value is 2×10^{30}, 1×10^{28} and 3×10^{25} cm^{-3} s for $a = 0.3, 0.1$ and 0.03 μm, respectively.

(iii) At high n_H/ζ, where grains are the dominant charged particles, the abundances of charged grains are nearly proportional to a^{-2} as long as the grain–grain collision is infrequent. At still higher n_H/ζ, where the neutralization by the grain–grain collision is efficient, the abundance of charged grains hardly depends on a.

Such general features are common to the other cases of the element depletion.

3   THE TIME-SCALE OF MAGNETIC FLUX LOSS

As shown in Section 2 the gas in the interstellar cloud is only slightly ionized. The dissipation processes of magnetic fields

in such clouds have been investigated comprehensively by Nakano (1984) and Nakano & Umebayashi (1986a). The electric field **E** in the local plane perpendicular to the magnetic field **B** is expressed as

$$\mathbf{E} + \frac{1}{c}(\mathbf{u}_n + \mathbf{v}_B) \times \mathbf{B} = 0, \tag{7}$$

where $\mathbf{u}_n$ is the velocity of neutral molecules in the inertial system and c is the light velocity. We call $\mathbf{v}_B$ the drift velocity of magnetic field because the magnetic flux through an arbitrary closed curve is conserved when every point on the curve moves with the velocity $\mathbf{v}_B$ relative to the neutrals. The components of this velocity are given by

$$v_{Bx} = \frac{A_1}{A} \frac{1}{c} |\mathbf{j} \times \mathbf{B}|, \tag{8}$$

$$v_{By} = -\frac{A_2}{A} \frac{1}{c} |\mathbf{j} \times \mathbf{B}|, \tag{9}$$

where $\mathbf{j} = (c/4\pi)\nabla \times \mathbf{B}$ is the electric current density,

$$A_1 = \sum_\nu \frac{\rho_\nu \omega_\nu^2}{\tau_\nu \Omega_\nu^2}, \qquad A_2 = \sum_\nu \frac{\rho_\nu \omega_\nu}{\tau_\nu^2 \Omega_\nu^2}, \tag{10}$$

$$A = A_1^2 + A_2^2 = \sum_{\kappa,\nu} \frac{\rho_\kappa \omega_\kappa}{\tau_\kappa^2 \Omega_\kappa^2} \frac{\rho_\nu \omega_\nu}{\tau_\nu^2 \Omega_\nu^2} (\tau_\kappa \omega_\kappa \tau_\nu \omega_\nu + 1), \tag{11}$$

$$\Omega_\nu^2 = \frac{1}{\tau_\nu^2} + \omega_\nu^2, \tag{12}$$

ρ_ν, τ_ν and $\omega_\nu = q_\nu eB/m_\nu c$ are the mass density, the viscous damping time of motion relative to the neutrals and the cyclotron frequency, respectively, of a particle ν with mass m_ν and electric charge $q_\nu e$. In equations (8) and (9) we have adopted the local Cartesian coordinates (x, y, z) with the z-axis along **B** and the x-axis along the magnetic force $(1/c)$ $(\mathbf{j} \times \mathbf{B})$. It is to be noticed that both components of the drift velocity are proportional to the strength of the magnetic force.

In general the dissipation of magnetic field is determined by v_{Bx} (Nakano & Umebayashi 1986a). This is self-evident for an axisymmetric cloud because the drift in the azimuthal (y) direction has no effect on the flux loss. When v_{Bx} is much smaller than the velocity u_{nx} of the neutrals, the magnetic field is nearly frozen to the neutral gas. When v_{Bx} is comparable to or greater than u_{nx}, the field is effectively decoupled from the gas.

The drift velocity v_{Bx} contains both the effects of the plasma drift and the ohmic dissipation. The ratio of the plasma drift to the ohmic dissipation is effectively given by (Nakano & Umebayashi 1986a)

$$D = \frac{1}{A} \sum_{\kappa,\nu} \frac{\rho_\kappa \omega_\kappa}{\tau_\kappa^2 \Omega_\kappa^2} \frac{\rho_\nu \omega_\nu}{\tau_\nu^2 \Omega_\nu^2} [\tau_\kappa \omega_\kappa (\tau_\nu \omega_\nu)^3 - 1]. \tag{13}$$

When positive and negative charges concentrate individually into a single species (which we denote κ and ν), equation (13) reduces to

$$D \approx -\tau_\kappa \omega_\kappa \tau_\nu \omega_\nu. \tag{14}$$

Thus, as long as $|\tau_e \omega_e \tau_i \omega_i| > 1$ and $n_e \approx n_i \gg n_g$, the magnetic field is mainly dissipated by the plasma drift. When the dominant charged particles are weakly coupled with the magnetic field, the ohmic dissipation overwhelms the plasma drift.

A magnetized cloud is usually non-spherical, contracted along the field lines. Let us consider an oblate cloud with mass M, radius R, half-thickness $Z(<R)$ and mean density

$$\rho \approx \frac{3M}{4\pi R^2 Z}. \tag{15}$$

Because the contraction along the field lines is faster than across the field, the cloud can easily attain quasi-equilibrium along the field lines, i.e.

$$\frac{GM}{R^2}\rho \approx \frac{k_B T}{\mu m_H}\frac{\rho}{Z}, \tag{16}$$

where μ is the mean molecular weight of the gas. From equations (15) and (16) we have

$$Z \approx \left(\frac{3k_B T}{4\pi G \mu m_H \rho}\right)^{1/2}. \tag{17}$$

We also have the mean column density

$$\sigma \approx \left(\frac{4k_B T\rho}{\pi G \mu m_H}\right)^{1/2}. \tag{18}$$

Equation (18) gives the column density of an isothermal disc with infinite extent if ρ is set equal to half the central density of the disc.

If the field configuration is fixed, the mean magnetic force in the cloud is proportional to B^2, i.e.

$$\frac{1}{c}|\mathbf{j} \times \mathbf{B}| = \left(\frac{B}{B_c}\right)^2 \frac{1}{c}|\mathbf{j} \times \mathbf{B}|_c, \tag{19}$$

where B is the mean field strength in the cloud and B_c is the critical field with which the mean magnetic force balances with the gravity, i.e.

$$\frac{1}{c}|\mathbf{j} \times \mathbf{B}|_c \approx \frac{GM}{R^2}\rho. \tag{20}$$

From equations (16), (17), (19) and (20) we have

$$\frac{1}{c}|\mathbf{j} \times \mathbf{B}| \approx \left(\frac{B}{B_c}\right)^2 \left(\frac{4\pi G k_B T}{3\mu m_H}\right)^{1/2}\rho^{3/2}. \tag{21}$$

The flux loss time in such a cloud may be given by $t_B \approx R/v_{Bx}$. However, the contraction of a cloud is quite non-homologous. As shown by the numerical simulations on the quasi-static contraction of axisymmetric clouds induced by the plasma drift (Nakano 1979, 1982, 1983b), the contraction of the central region with higher density is faster than the outer region with lower density and forms a core, which finally begins dynamical contraction. The time-scale of such a non-homologous process is given by the time in which the magnetic field drifts the scalelength of the central region which is of the order of Z. Thus we define the dissipation time of the magnetic field as

$$t_B \approx Z/v_{Bx}. \tag{22}$$

From equations (8), (17), (21) and (22) we have

$$t_B \approx \left(\frac{B_c}{B}\right)^2 \frac{A}{A_1}\frac{3}{4\pi G \rho^2}. \tag{23}$$

The efficiency of magnetic field dissipation can be found by comparing t_B with the free-fall time $t_f = (3\pi/32 G\rho)^{1/2}$.

The critical field B_c can be determined from equations (1), (16) and (17) as

$$B_c \approx 4\left(\frac{\pi k_B T\rho}{3\mu m_H}\right)^{1/2}. \tag{24}$$

Substituting this into equation (21) we find that the scale-length H of the magnetic field defined by

$$\frac{1}{c}|\mathbf{j} \times \mathbf{B}| \approx \frac{B^2}{4\pi H} \tag{25}$$

is nearly equal to $4Z/3$. The critical field may be defined in a different way. An isothermal gaseous disc penetrated by a uniform magnetic field perpendicular to the disc layer is gravitationally unstable only when B is smaller than the critical field (Nakano & Nakamura 1978)

$$B_c \approx 2\pi G^{1/2}\sigma. \tag{26}$$

This equation has a similar meaning as equation (1). This critical field is $\sqrt{3}$ times greater than equation (24) and the corresponding scalelength H is 3 times greater than the above. However, when the dominant charged particles are strongly coupled with the magnetic field, i.e. $|\tau_\nu \omega_\nu| \gg 1$, A/A_1 hardly depends on B (e.g. when charged grains are negligible, we have $A/A_1 \approx \rho_i/\tau_i$). In such a situation t_B for a given value of B/B_c hardly depends on the choice of B_c. In the following we adopt equation (24) as B_c. We are mainly concerned with the cases of $B \lesssim B_c$, because the cloud with $B > B_c$ expands and does not form stars.

We shall investigate the clouds of mean hydrogen density n_H up to 10^{13} cm^{-3}. Because the grain opacity for the radiation of 10 K is about 0.01 cm^2 g^{-1} (Hayashi & Nakano 1965), clouds with $n_H \lesssim 10^{13}$ cm^{-3} are almost transparent as seen from equation (18). We therefore take $T \approx 10$ K. In calculating the densities of the charged particles, we use the ionization rate of a hydrogen molecule in the cloud core

$$\zeta \approx \zeta_{CR}\exp\left(-\frac{\sigma}{2\chi}\right) + \zeta_R, \tag{27}$$

where $\zeta_{CR} \approx 1 \times 10^{-17}$ s^{-1} and $\zeta_R \approx 6.9 \times 10^{-23}$ s^{-1} are the ionization rates by cosmic rays in the interstellar space and by the radioactive elements in the cloud, respectively, and $\chi \approx 96$ g cm^{-2} is the attenuation length of the ionization rate (Umebayashi & Nakano 1981). As seen from equation (18), the attenuation of cosmic rays is efficient at $n_H \gtrsim 10^{12}$ cm^{-3}.

Figs 7 and 8 show the results for the case of $\delta_1 = \delta_2 = 0$ with $a = 0.1$ μm. The solid curves in Fig. 7 show the contours of constant t_B/t_f on the (n_H, B) plane, and the solid curves in Fig. 8 show the contours of constant D, the efficiency ratio of the plasma drift to the ohmic dissipation given by equation (13). In both figures the critical field strength B_c given by equation (24) is shown by the dot-dashed lines, and the field strengths for the state of $|\tau_\nu \omega_\nu| = 1$ for electrons, dominant ions and grains of charge $\pm e$ are shown by the dashed lines.
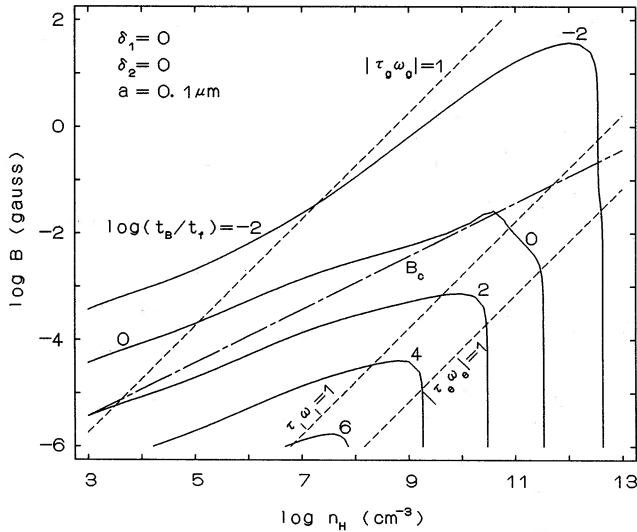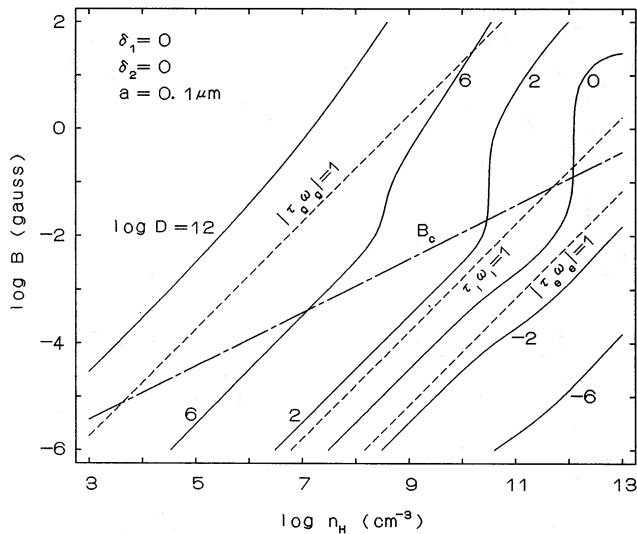
Figure 7. The dissipation time t_B of magnetic fields in the core of an oblate cloud as a function of the mean density n_H and the mean field strength B for $\delta_1 = \delta_2 = 0$ and for $a = 0.1$ μm. The solid curves represent the contours of constant t_B/t_f and are labelled with the values of log (t_B/t_f) where $t_f = (3\pi/32G\rho)^{1/2}$ is the free-fall time. The dot-dashed line represents the critical field strength B_c for contraction given by equation (24). The dashed lines represent the field strength for the state $|\tau_\nu\omega_\nu| = 1$ for electrons, dominant ions and grains with electric charge $\pm e$.

Figure 8. The ratio of the effects of plasma drift and ohmic dissipation D defined by equation (13) in the core of an oblate cloud as a function of the mean density n_H and the mean field strength B for $\delta_1 = \delta_2 = 0$ and for $a = 0.1$ μm. The solid curves represent the contours of constant D and are labelled with the values of log D. The critical field strength B_c and the state of $|\tau_\nu\omega_\nu| = 1$ are shown by the dot-dashed and the dashed lines, respectively.

Some of the qualitative features of the results at $n_H \lesssim 10^{11}$ cm^{-3} can be obtained from the following consideration. For $\tau_i\omega_i \gtrsim 1$ and $|\tau_g\omega_g| \lesssim 1$, which are satisfied at least at $B \approx B_c$ and $n_H \approx 10^3$–10^{11} cm^{-3}, we obtain from equations (10)–(12) and (23)

$$t_B \approx \left(\frac{B_c}{B}\right)^2 \frac{3}{4\pi G\rho^2} \frac{(\rho_i/\tau_i)^2 + (\rho_g\omega_g)^2}{(\rho_i/\tau_i) + \rho_g\tau_g\omega_g^2}, \tag{28}$$

though the error may be as large as a factor of 2 in some situations. At $n_H \lesssim 10^{11}$ cm^{-3} and $B \lesssim B_c$ with $a = 0.1$ μm, the terms due to grains are minor. In such a situation t_B is proportional to the ionization fraction ρ_i/ρ and inversely proportional to B^2 because $\tau_i \propto \rho^{-1}$. Hence, as B increases at a given n_H, t_B decreases. However, even at $B = B_c$, t_B is greater than $6t_f$ at $n_H \lesssim 10^8$ cm^{-3} and greater than t_f at $10^8 \lesssim n_H \lesssim 4 \times 10^{10}$ cm^{-3} as seen from Fig. 7. Because $t_B \propto (B_c/B)^2 \propto (\Phi_c/\Phi)^2$ and the cloud with $\Phi < \Phi_c$ contracts nearly freely as long as its mass is somewhat greater than the Jeans mass, it is difficult to decrease the flux far below Φ_c at these densities.

When $D \ll 1$, t_B is nearly independent of B. This is characteristic of ohmic dissipation: the ohmic dissipation time is given by $4\pi\sigma_c H^2/c^2$ independent of B, where σ_c is the electric conductivity.

At $n_H >$ several $\times 10^{11}$ cm^{-3} we have $t_B < t_f$ for any B as seen from Fig. 7. Because the dynamical evolution of the cloud usually cannot proceed faster than the free fall, the magnetic field is decoupled from the gas at these densities. However, this does not mean that the magnetic field of any configuration cannot exist in the cloud. The field with the scalelength H much greater than the scalelength of the cloud Z (e.g. a nearly uniform field) can exist though it hardly couples with the gas.

The qualitative features are nearly the same for the other cases of element depletion. Fig. 9 shows t_B at $B = B_c$ for the three cases of element depletion. At $n_H \lesssim 4 \times 10^{10}$ cm^{-3} t_B is greater than t_f for all cases, and the magnetic field decouples from the gas for any B only at $n_H \gtrsim$ several $\times 10^{11}$ cm^{-3}. Nakano (1988a) obtained t_B somewhat greater than those shown in Fig. 9 especially in the case of $\delta_1 = 0.2$ and $\delta_2 = 0$ where the ion density is the lowest. This is because he took n_g/n_H about 4 times greater considering the existence of icy materials and then the grain term in the numerator of equation (28) is not negligible. In Section 4 we shall calculate t_B with ice-mantled grains.

Although we have assumed that all grains have the same radius $a = 0.1$ μm, the grain size spreads in a wide range. To find the effect of grain size we have investigated the cases of $a = 0.3$ and 0.03 μm. Fig. 10 shows t_B in the state of $B = B_c$ with $a = 0.3$ μm. Although the curves for t_B behave nearly the same as in Fig. 9, t_B is considerably greater in some density range. This is because the recombination on grains is less efficient and then the ion density is higher. Fig. 11 shows t_B in the state of $B = B_c$ with $a = 0.03$ μm. The curves for t_B have plateaus at $n_H \approx 10^5$–10^9 cm^{-3}. In the case of $a = 0.03$ μm $|\omega_g|$ is 37 times greater than in the case of $a = 0.1$ μm. The smaller grain radius also makes the ion density lower. Thus the term due to grains in the numerator of equation (28) is greater than the term due to ions in this density range, while in the denominator the two terms are comparable and the ratio of the two terms is nearly constant. Because $\rho_g \propto \rho$, $\omega_g^2 \propto B_c^2 \propto \rho$, $\rho_i \approx$ constant and $\tau_i \propto \rho^{-1}$, we have $t_B \approx$ constant or a plateau in this density range. At $n_H \gtrsim 10^9$ cm^{-3} the fraction of charged grains ρ_g/ρ decreases with the density and then t_B decreases. At $n_H \lesssim 10^5$ cm^{-3} the ion term in the numerator of equation (28) is dominant and then the behaviour of t_B is similar to the case of $a = 0.1$ μm. At
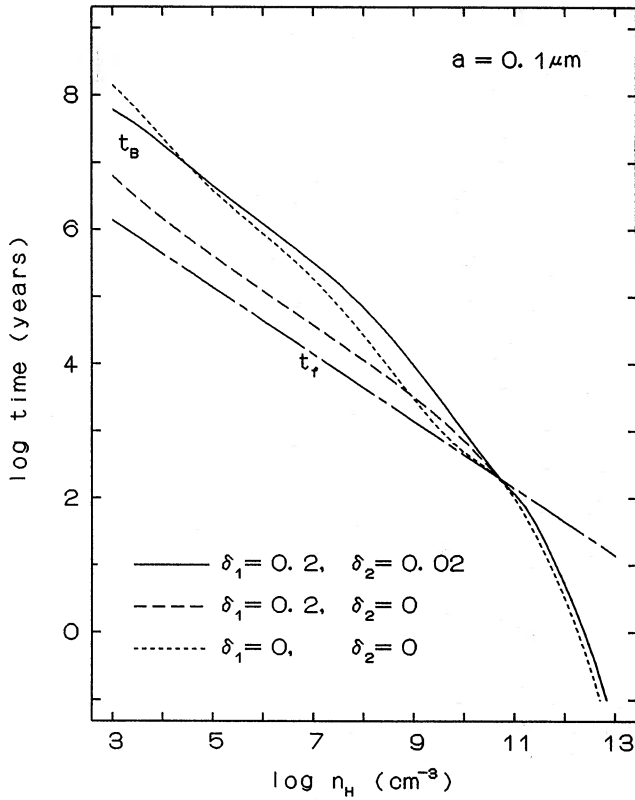
Figure 9. The time-scale of magnetic flux loss in the core of an oblate cloud with $a = 0.1$ μm for three cases of the depletion of heavy elements; the full line is for $\delta_1 = 0.2$ and $\delta_2 = 0.02$, the dashed line is for $\delta_1 = 0.2$ and $\delta_2 = 0$, and the dotted line is for $\delta_1 = \delta_2 = 0$. The free-fall time t_f is also shown for comparison.

Figure 10. The time-scale of magnetic flux loss in the core of an oblate cloud with $a = 0.3$ μm for three cases of the depletion of heavy elements. The other details are the same as in Fig. 9.

$n_H \lesssim 4 \times 10^{10}$ cm^{-3}, t_B is greater than $4t_f$ for all the cases of element depletion. The magnetic field decouples from the gas only at $n_H \gtrsim$ several $\times 10^{11}$ cm^{-3} as in the other cases of grain size.

4 DISCUSSION

In determining the densities of charged particles in Sections 2 and 3 we assumed that the gas is in ionization–recombination equilibrium. This assumption holds when the relaxation time of each kind of charged particles to an equilibrium state is much smaller than the evolutionary time-scale of the cloud. From equation (4) the time-scale $t_1(X_i)$ in which the particle X_i approaches the ionization–recombination equilibrium is approximately given by the minimum of

$$\left| \frac{n(X_i)}{\beta_{ijk} n(X_j) n(X_k)} \right|. \tag{29}$$

We estimate $t_1(X_i)$ by using the equilibrium abundances of charged particles used in Section 3. The results for the case of $\delta_1 = \delta_2 = 0$ and $a = 0.1$ μm are shown in Fig. 12. The time-scales $t_1(X_i)$ for some kinds of particles are shown by solid lines and the viscous damping times τ_ν of electron, H$_3^+$ and grains are shown by dashed lines. The free-fall time t_f is also shown by a dot–dashed line. Because $t_1(X_i) \ll t_f$ for all particles, we can regard the gas as being in ionization–recombi-
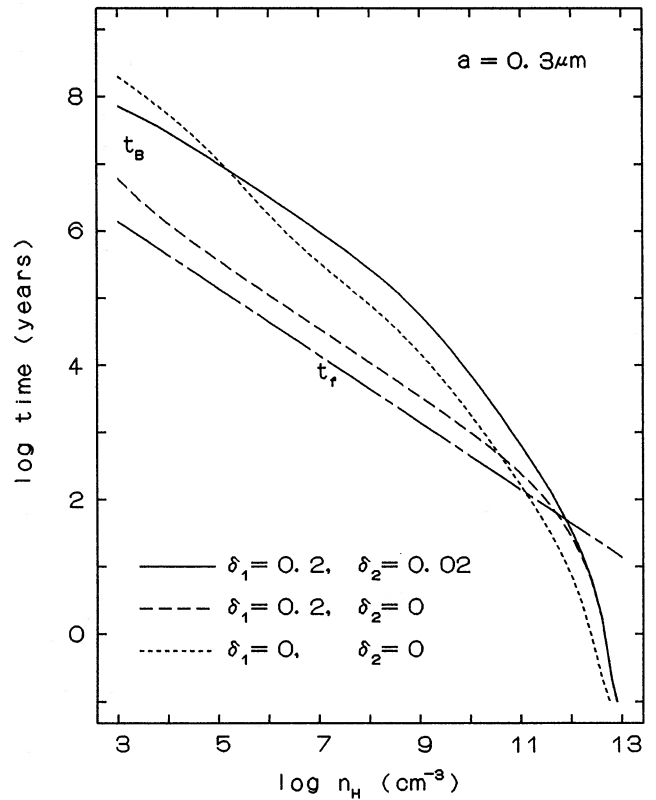

Figure 11. The time-scale of magnetic flux loss in the core of an oblate cloud with $a = 0.03$ μm for three cases of the depletion of heavy elements. The other details are the same as in Fig. 9.
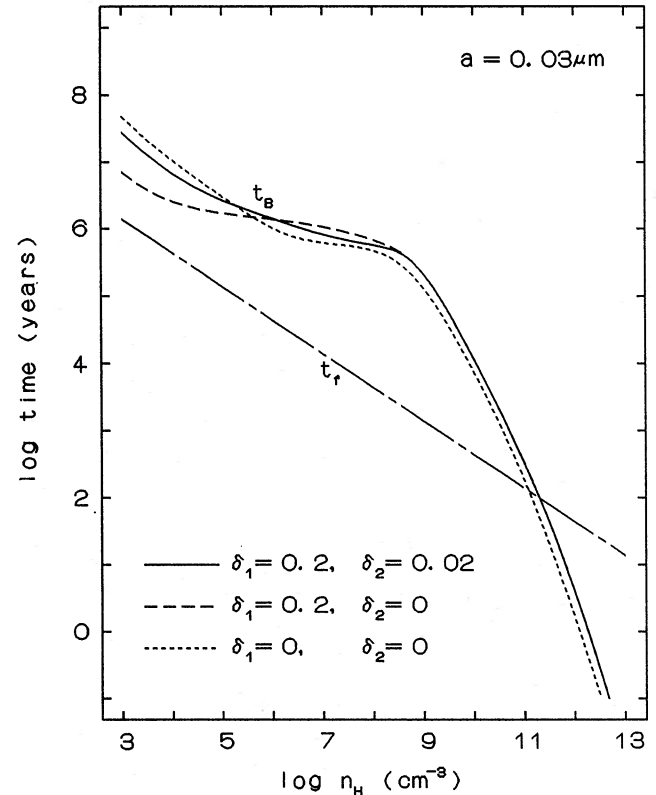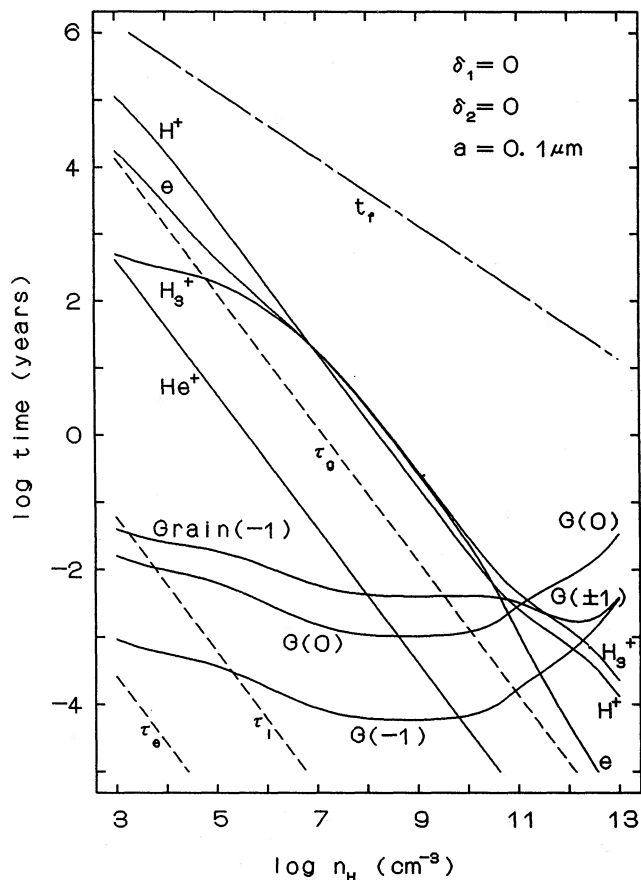
Figure 12. The relaxation time to the ionization–recombination equilibrium for various charged particles in the core of an oblate cloud (solid curve). We have taken $\delta_1 = \delta_2 = 0$ and $a = 0.1$ μm. The dashed lines show the viscous damping times of motion relative to neutrals τ_v for electron, ion H_3^+ and grain. The free-fall time t_f is shown by a dot–dashed line.

nation equilibrium at the densities considered in this paper. The situation is similar for the other cases of element depletion.

Because the relaxation time t_I for ions and electrons is much greater than the viscous damping times τ_i and τ_e, we can neglect the effects of the change of the charge state on the motion of ions and electrons. The time-scales of charge change of grains are much smaller than τ_g at $n_H \lesssim 10^{10}$ cm^{-3}. Because the charge of a grain changes stochastically in τ_g, it must move in a complicated way (Elmegreen 1979). We have regarded each grain as having a fixed charge and the fraction of grains in each charge state is proportional to the mean duration time of the state. This is a good approximation as discussed by Nakano & Umebayashi (1980, 1986a).

In Sections 2 and 3 we neglected the existence of icy materials such as H_2O, CH_4 and NH_3 in grains. The inclusion of such materials would enhance the grain size and/or the number of grains. To clarify the effect of the existence of icy materials, we have investigated the following two cases: (A) $a = 0.22$ μm and $n_g/n_H = 8.9 \times 10^{-13}$; (B) $a = 0.1$ μm and $n_g/n_H = 8.8 \times 10^{-12}$. The inner density of icy materials in grains has been taken 0.9 g cm^{-3} in both cases. In case A, t_B is nearly the same as in the case of $a = 0.1$ μm without icy

materials shown in Fig. 9. In case B, t_B is enhanced considerably compared with those in Fig. 9 especially at $10^8 \lesssim n_H \lesssim 4 \times 10^{10}$ cm^{-3} and is similar to those in Fig. 11.

By the coalescence of grains the grain radius may increase and the relative number density of grains may decrease as n_H increases. However, as seen by comparing Figs 9 and 10, t_B cannot be smaller than in the case of $a = 0.1$ μm. Furthermore, the coalescence occurs frequently only at $n_H \gtrsim 10^{13}$ cm^{-3} if they collide with their thermal velocity. Thus the coalescence has no important effects on the behaviour of magnetic fields.

In Sections 2 and 3 we have assumed for simplicity that all grains have the same size and investigated the three cases of the grain radius $a = 0.3$, 0.1 and 0.03 μm. In reality, however, the interstellar grains have a wide size distribution, e.g. between 0.25 and 0.005 μm (Mathis, Rumple & Nordsieck 1977). From the results in Section 3 showing that the case of $a = 0.1$ μm gives the minimum t_B, we can make the following estimation. If we shift some of the grains to the size larger than 0.1 μm fixing the total grain abundance ρ_g/ρ, the total surface area of grains decreases and the ion density increases. This has an effect of increasing t_B. Because a larger grain couples with magnetic fields more weakly, the shift to larger size also has an effect of decreasing t_B. However, the latter effect is smaller because the contribution of grains with $a = 0.1$ μm to t_B is already small compared with the ions. If we shift some of the grains to the size somewhat smaller than 0.1 μm, the total surface of grains increases and the ion density decreases, which has an effect of decreasing t_B. The shift to smaller size also has an effect of increasing t_B because smaller grains couple with magnetic fields more strongly. The results for the cases of $a = 0.1$ and 0.03 μm show that the latter effect is dominant. Thus we can say that t_B cannot be smaller than in the case of $a = 0.1$ μm shown in Figs 7 and 9. Because there are many interstellar grains with $a \ll 0.1$ μm, t_B must be considerably greater than in the case of $a = 0.1$ μm. Thus t_B is considerably greater than t_f at $n_H < 10^{11}$ cm^{-3}, and the magnetic field decouples from the gas only at $n_H \gtrsim$ several $\times 10^{11}$ cm^{-3}.

The magnetic flux loss in the gaseous discs permeated by magnetic field parallel to the disc layer has been investigated by many authors (Shu 1983; Paleologou & Mouschovias 1983; Scott 1984; Mouschovias, Paleologou & Fiedler 1985; Nakano 1985) by assuming the gas moving only perpendicularly to the layer. Some of the results for such discs are quite different from those shown in Section 3. For instance, Mouschovias *et al.* (1985) found that the magnetic flux decreases by several orders of magnitude at $n_H \ll 10^{11}$ cm^{-3}. Such a disc in hydrostatic equilibrium has a central pressure $P_c = \pi G\sigma^2/2$, where σ is the column density of the disc. If the magnetic pressure overwhelms the gas pressure, the magnetic force nearly balances the gravity and then the magnetic flux is lost in a time-scale considerably greater than t_f as in the cloud with $B \approx B_c$ investigated in Section 3. After the disc has lost some magnetic flux, it contracts until the pressure recovers the equilibrium value. If the magnetic pressure is still dominant in this state, the disc again loses its flux in a time-scale considerably greater than the free-fall time at this new state. The disc repeats this process until the gas pressure becomes dominant. Thus such a disc can lose its magnetic flux by orders of magnitude in a time-scale considerably greater than the initial free-fall time.

Mouschovias *et al.* (1985) seem to have simulated such a process in some of their models.

However, such a disc is gravitationally unstable and breaks into fragments in a free-fall time (Nakano 1988b). Before significant magnetic flux is lost, the disc transforms itself into a quite different configuration contracted along the field lines (Nakano 1985). The magnetic flux loss investigated in Section 3 is for clouds with such configuration. Although a disc with parallel magnetic field can provide properly the time-scale of flux loss, one cannot predict the total amount of the flux lost.

5 CONCLUSIONS

We have investigated the densities of charged particles and the dissipation of magnetic field in the interstellar clouds of density $n_H = 10^3 - 10^{13}$ cm^{-3} with some new rate coefficients of reactions. Especially the dissociative recombination rate of H_3^+ with an electron has been decreased by a factor of 10^2 compared to the rate generally used previously. The main results are as follows.

(i) By the reactions with CO, O_2 and O, H_3^+ is transformed into other molecular ions. Even if there is no C or O in the gas phase, H_3^+ recombines with an electron on the grain surface. Therefore, the great decrease in the dissociative recombination rate of H_3^+ does not enhance the ion density so much.

(ii) At $n_H \lesssim 10^{11}$ cm^{-3} the magnetic flux loss time t_B in the core of an oblate cloud is considerably greater than the free-fall time when the cloud core has the critical magnetic field B_c with which the magnetic force balances gravity. Because $t_B \propto (B_c/B)^2$ as long as the plasma drift (ambipolar diffusion) overwhelms the ohmic dissipation and the core with $B < B_c$ contracts nearly freely as long as its mass is somewhat greater than the Jeans mass, it is difficult to decrease the magnetic flux greatly at these densities.

(iii) At $n_H \gtrsim$ several $\times 10^{11}$ cm^{-3}, t_B is less than the free-fall time irrespective of the field strength as long as the scale-length of magnetic field is nearly equal to the size of the cloud core. Thus the magnetic field is decoupled from the gas and only a nearly uniform field with scalelength much greater than the size of the core can exist.

REFERENCES

Amano, T., 1988. *Astrophys. J.*, **329**, L121.
Cameron, A. G. W., 1982. *Essays in Nuclear Astrophysics*, p. 23, eds Barnes, C. A., Schramm, D. N. & Clayton, D. D., Cambridge University Press, Cambridge.
Capone, L. A., Whitten, R. C., Dubach, J., Prasad, S. S. & Huntress, W. T., Jr., 1976. *Icarus*, **28**, 367.
Draine, B. T. & Sutin, B., 1987. *Astrophys. J.*, **320**, 803.
Elmegreen, B. G., 1979. *Astrophys. J.*, **232**, 729.
Field, G. B., 1970. *Mem. Soc. R. Sci. Liège*, **19**, 29.
Hayashi, C. & Nakano, T., 1965. *Progr. Theor. Phys.*, **34**, 754.
Mathis, J. S., Rumpl, W. & Nordsieck, K. H., 1977. *Astrophys. J.*, **217**, 425.
Mestel, L., 1965. *Q. Jl R.astr. Soc.*, **6**, 265.
Mestel, L., 1966. *Mon. Not. R. astr. Soc.*, **133**, 265.
Mestel, L. & Spitzer, L., Jr., 1956. *Mon. Not. R. astr. Soc.*, **116**, 503.
Michels, H. H. & Hobbs, R. H., 1984. *Astrophys. J.*, **286**, L27.
Mitchell, G. F., Ginsburg, J. L. & Kuntz, P. J., 1978. *Astrophys. J. Suppl.*, **38**, 39.
Morton, D. C., 1974. *Astrophys. J.*, **193**, L35.
Mouschovias, T. Ch., Paleologou, E. V. & Fiedler, R. A., 1985. *Astrophys. J.*, **291**, 772.
Nakano, T., 1976. *Publs astr. Soc. Japan*, **28**, 355.
Nakano, T., 1979. *Publs astr. Soc. Japan*, **31**, 697.
Nakano, T., 1981. *Progr. Theor. Phys. Suppl., No. 70*, 54.
Nakano, T., 1982. *Publs astr. Soc. Japan*, **34**, 337.
Nakano, T., 1983a. *Publs astr. Soc. Japan*, **35**, 87.
Nakano, T., 1983b. *Publs astr. Soc. Japan*, **35**, 209.
Nakano, T., 1984. *Fundam. Cosmic Phys.*, **9**, 139.
Nakano, T., 1985. *Publs astr. Soc. Japan*, **37**, 69.
Nakano, T., 1988a. *Galactic and Extragalactic Star Formation*, p. 111, eds Pudritz, R. E. & Fich, M., Kluwer, Dordrecht.
Nakano, T., 1988b. *Publs astr. Soc. Japan*, **40**, 593.
Nakano, T. & Nakamura, T., 1978. *Publs astr. Soc. Japan*, **30**, 671.
Nakano, T. & Umebayashi, T., 1980. *Publs astr. Soc. Japan*, **32**, 613.
Nakano, T. & Umebayashi, T., 1986a. *Mon. Not. R. astr. Soc.*, **218**, 663.
Nakano, T. & Umebayashi, T., 1986b. *Mon. Not. R. astr. Soc.*, **221**, 319.
Oppenheimer, M. & Dalgarno, A., 1974. *Astrophys. J.*, **192**, 29.
Paleologou, E. V. & Mouschovias, T. Ch., 1983. *Astrophys. J.*, **275**, 838.
Prasad, S. S. & Huntress, W. T., Jr., 1980. *Astrophys. J. Suppl.*, **43**, 1.
Scott, E. H., 1984. *Astrophys. J.*, **278**, 396.
Shu, F. H., 1983. *Astrophys. J.*, **273**, 202.
Smith, D. & Adams, N. G., 1984. *Astrophys. J.*, **284**, L13.
Strittmatter, P. A., 1966. *Mon. Not. R. astr. Soc.*, **132**, 359.
Umebayashi, T., 1983. *Progr. Theor. Phys.*, **69**, 480.
Umebayashi, T. & Nakano, T., 1980. *Publs astr. Soc. Japan*, **32**, 405.
Umebayashi, T. & Nakano, T., 1981. *Publs astr. Soc. Japan*, **33**, 617.